Soft-Etch Mesoporous Hole-Conducting Block Copolymer Templates

Edward J. W. Crossland,[†,‡] Pedro Cunha,[†] Steve Scroggins,[§] Stephen Moratti,[¶] Olena Yurchenko,[∥] Ullrich Steiner,[†,‡] Marc A. Hillmyer,[⊥] and Sabine Ludwigs[‡,∥,]*

[†]Cavendish Laboratory, J. J. Thomson Avenue, University of Cambridge, Cambridge CB3 0HE, U.K., [‡]Freiburg Institute for Advanced Studies (FRIAS), University of Freiburg, 79104 Freiburg, Germany, [§]Division of Materials Sciences, Lawrence Berkeley National Laboratory and College of Chemistry, University of California, Berkeley, California 94720, [¶]Department of Chemistry, University of Otago, Dunedin, New Zealand, [∥]Freiburg Materials Research Center and Institute for Macromolecular Chemistry, University of Freiburg, Stefan-Meier-Str. 21, 79104 Freiburg, Germany, and [⊥]Department of Chemistry, University of Minnesota, Minneapolis, Minnesota 55455

ABSTRACT We present a mesoporous hole-conducting polymer film resulting from spontaneous block copolymer self-assembly based on a simple spin-coating protocol. A diblock copolymer consisting of a triphenylamine side group polymer and a poly(D,L-lactide) block (PSTPA-*b*-PLA) is shown to microphase separate to form ordered 13 nm cylindrical PLA microdomains embedded in the semiconducting PSTPA matrix. Partially ordered and film-spanning PLA domains could be identified in films immediately after spin coating from toluene solutions on conducting substrates. Selective mild etching of the minority PLA domains (in weak aqueous base) leads to a mesoporous hole-conducting polymer matrix. The pore structure is replicated electrochemically in platinum, demonstrating the viability of this approach to producing nano-organized heterojunction structures in thin films.

*Address correspondence to
sabine.ludwigs@makro.uni-freiburg.de.

The ordered, periodic structures produced by the self-assembly of diblock copolymers offer an ideal toolbox for applications in nanotechnology that demand intimate interdigitation of functional materials such as in donor—acceptor semiconductor bulk heterojunction solar cells. A continuous and distributed interdigitation of donor—acceptor (D—A) phases on the 10 nm length scale is needed to facilitate interfacial exciton dissociation throughout the active layer of a device while maintaining charge transport pathways through each material to external electrodes.

A grand challenge in the application of block copolymer self-assembly in photovoltaic devices is to reproduce the idealized nanostructures found in model (non-semiconducting) materials in functional D—A materials and to orient these structures to produce a vertical interdigitation in a thin film device geometry. A recent review of progress in photovoltaic applications of block copolymer can be found in ref 1. Several groups have demonstrated the possibility of tethering functional do-

nor polymers such as poly(alkyl thiophenes) to insulating blocks and have achieved microphase-separated structures.[2−4] Direct synthesis of a processable donor—acceptor diblock copolymer demands significant synthetic efforts but has been demonstrated.[5−12] An alternative approach is to attach a minority sacrificial block to a desirable functional majority polymer, whose sole purpose is to direct the microphase morphology of the functional material. If the sacrificial block is chosen to be degradable *via* "soft" chemical processing (*i.e.*, without damage to the functional phase), its subsequent removal leaves a functional matrix with well-defined mesoporosity. This strategy has been applied to nonfunctional block copolymers that were used as templates for the growth of nanostructured TiO₂ for dye-sensitized solar cells.[13,14] Boudouris *et al.* have recently reported on the synthesis, microphase separation, and etching of polythiophene-*block*-polylactide block copolymers.[15] In recent work, Botiz and Darling used related nanoporous templates for the deposition of electron-accepting fullerenes.[16] Significantly, the choice of complementary component is not limited to polymeric materials synthetically compatible with the primary polymer. A wide selection of electrodeposited inorganic semiconductors, nanoparticles, or small molecules can potentially be infiltrated into the prestructured layer.

We have synthesized a block copolymer, termed PSTPA-*b*-PLA, with a hole-transporting majority block made up of redox-active triphenylamine (TPA) side groups attached to a polystyrene (PS) backbone *via* flexible ether linkages and a minority poly(D,L-lactide) (PLA) block. Hole-

conducting properties of TPA side group polymers have been reported.[9,17] Snaith *et al.* have demonstrated the utility of these homopolymers as the donor phase in mesostructured heterojunction solar cells based on polymer brushes infiltrated with CdSe nanoparticle acceptors.[18,19] The second minority component (PLA) is susceptible to mild hydrolytic degradation in aqueous base[20,21] and is designed to introduce well-defined, ~10 nm diameter cylindrical pores to the semiconducting matrix.

We found spontaneous formation of a film-spanning and microphase-separated PLA minority domain structure immediately after spin coating of block copolymer thin films on Au-coated silicon substrates. The PLA component was successfully removed to produce mesoporous polymeric hole conductor films with 10 nm pores. We demonstrate that electrochemical deposition can be used to fill the internal pore structure, which penetrates the full thickness of the film, such that both material phases can provide continuous charge extraction pathways to external electrodes. We plan, ultimately, to infiltrate strongly absorbing acceptor phases such as CdSe into the mesoporous PSTPA film to produce efficient bulk heterojunction hybrid photovoltaic devices.

RESULTS AND DISCUSSION

The synthesis of the PSTPA-*b*-PLA block copolymer by RAFT and ring-opening polymerization is summarized in Figure 1 and described in detail in the Supporting Information.

The absorption maximum of the block copolymer in the neutral state was 302 nm in chloroform solution and is identical to the absorption of the corresponding monomer triphenylamine.[22] While the polymer alone shows rather short wavelength absorption to effectively cover the solar spectrum, this offers the opportunity to couple with an infiltrated acceptor absorbing in the red (for example, CdSe) giving a broad overall cell absorption. The charge transport mobility of a PSTPA homopolymer film (*h*-PSTPA) was probed in bottom gate, bottom contact thin film field-effect transistors. A hole mobility of $\mu_{PSTPA} = 1 \times 10^{-5}$ cm^2 V^{-1} s^{-1} was measured in the saturation regime (transistor characteristics are included in Supporting Information). Cyclic voltammetry showed, in accordance with literature,[9,17,23] a HOMO level for the PSTPA of −5.21 eV, which further increased to −5.02 eV following irreversible dimerization of TPA groups upon *in situ* electrochemical oxidation (see Supporting Information).

We studied three block copolymers containing between 60 and 70 wt % of the PSTPA component as to target cylinders of PLA in a matrix of PSTPA. Morphological data shown here are taken from the copolymer PSTPA-*b*-PLA(I) with a M_n of 30.9 kg mol^{-1} (determined by NMR spectroscopy) containing 62 wt % PSTPA and with a polydispersity index of 1.35 (determined by SEC). All three copolymers showed identical microphase be-
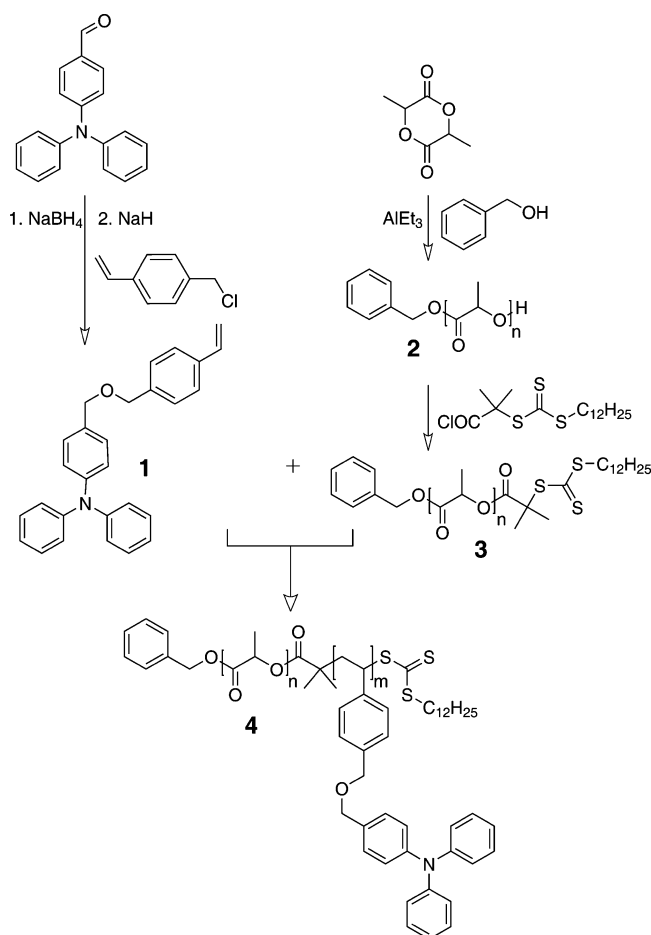

Figure 1. Synthesis of PSTPA-*b*-PLA.

havior. The films were spin-coated from 10 wt % toluene solutions onto gold-coated silicon substrates. The copolymer microphase morphology was first investigated by thermally annealing thin copolymer films under inert atmosphere at 140 °C above the glass transition temperatures of both components (T_g values from DSC are 52 and 69 °C for PLA and PSTPA, respectively). After cooling the films to room temperature, the PLA minority component was selectively etched by submersing the films in 0.05 M NaOH$_{(aq)}$ solutions containing 40 vol % methanol for several hours.

Films annealed both with an unconfined free surface and confined in a sandwich geometry consisting of a cross-linked poly(dimethylsiloxane) (PDMS) stamp pressed onto the upper surface resulted in a cylindrical microphase morphology lying parallel to the substrate. This morphology was confirmed by a combination of scanning force microscopy (SFM) height data and cross-sectional transmission electron microscopy (TEM) shown in Figure 2. The principle center-to-center spacing determined by Fourier transform of the surface SFM image is 27 ± 4 nm.

Parallel alignment of the block copolymer cylinder morphology in both free surface and surface-confined thin films is well-known and usually arises from asymmetric interaction energy of the two blocks with one or both
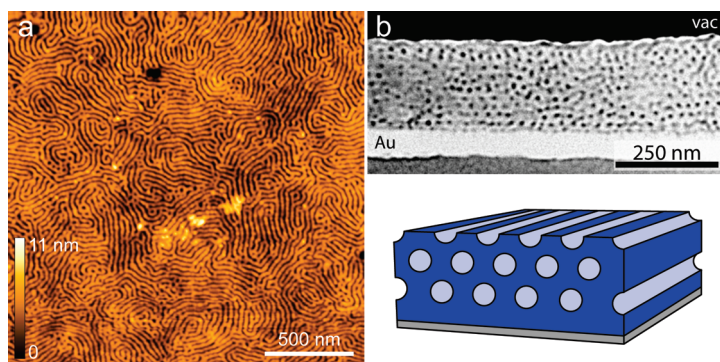
Figure 2. Thin film copolymer morphology. (a) Tapping-mode SFM (height data) image of a 240 nm PSTPA-*b*-PLA film annealed at 140 °C for 35 h followed by PLA etching. (b) Cross-sectional TEM (negative image, high electron density bright) and schematic of lying cylinder morphology. The PSTPA phase was stained with ruthenium tetroxide vapors to improve contrast.

confining interfaces. A vertical interdigitation of two materials, as required in the bulk heterojunction concept, demands a degree of perpendicular orientation of the copolymer morphology such that the minority cylindrical domains span continuously from top to bottom of the film. In fact, we found that the PSTPA-*b*-PLA copolymer can spontaneously adopt such a morphology after simple spin coating, without the need for further annealing. Figure 3a shows a scanning electron micrograph (SEM) of a 380 nm thick film (determined by SFM height measurements) following PLA removal immediately after spin coating. A well-ordered, hexagonally packed array of cir-
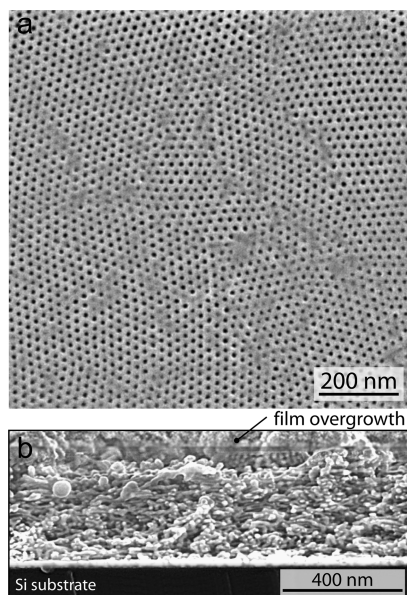

Figure 3. Porous PSTPA templates as formed immediately after spin coating from toluene solution. (a) Surface SEM image showing hexagonal ordering of pores in the PSTPA matrix after PLA removal (film thickness = 380 nm). Average pore diameter = 13 ± 2 nm, center-to-center spacing = 21 ± 2 nm. (b) Cross-sectional SEM view of electrochemical replication of the film in (a) with platinum followed by dissolving the PSTPA matrix in toluene. "Overgrowth" of platinum metal can be seen emerging at the top of the image. The replication indicates that the porous structure penetrates the full film thickness to the conducting Au substrate.

cular pores with a center-to-center distance of 21 ± 2 nm and an average diameter of 13 ± 2 nm indicates a perpendicular alignment of the cylindrical PLA domains at the free surface. The pore density is 1950 μm^{-2}. For comparison, the pore density in the unit cell of the hexagonal structure is 2000 μm^{-2}, consistent with a high degree of perpendicular orientation at the surface. Electrochemical deposition of platinum metal is an ideal probe of the continuity of the pore structure within the film. No electrochemical deposition was possible at all through films with parallel orientation of the cylinders, indicating that the nonporous PSTPA itself is an effective barrier for active species in the electrolyte. On the other hand, electrochemical deposition was possible through the pore structure in spin-coated films. The continuity of the pores is revealed by SEM of the freestanding conducting platinum nanostructures after simple dissolution of the PSTPA template (Figure 3b). A cross-section view of the nanostructure shows a densely packed network of platinum structures (*i.e.*, with no clear preferential orientation) that penetrate through the template to the conducting substrate.

A film-spanning microphase-separated PLA minority domain structure immediately after spin coating can be rationalized by comparison to observations of classical block copolymer thin film phase behavior. The morphology obtained by spin coating is far from equilibrium and kinetically trapped. Further thermal annealing leads to the equilibrium lying cylinder morphology demonstrated in Figure 2 and the tendency to form terraces in very thin films. Surprisingly, however, the morphology at the surface (Figure 3a) shows well-ordered hexagonally arranged holes. Although the microphase morphology in the center of the films lacks long-range order in either horizontal or vertical directions, the PLA domains certainly percolate through to the substrate. During spin coating, the initially spin-coated film is phase-mixed due to the presence of toluene, which is a good solvent for both blocks. In a dilute solution, the presence of solvent molecules mediates nonfavorable interactions between the immiscible blocks, resulting in a single disordered phase. After the flow-induced thinning of the film during spin coating, solvent evaporation from the layer causes a gradient in solvent concentration and therefore a disorder to order transition. Interfacial interactions are strongly mediated by the presence of solvent molecules in both phases, which mitigates preference of one of the blocks for the surface. This could explain the high order at the free surface. The rate of solvent evaporation and the resulting concentration gradients also influence the order and alignment of classical block copolymer films. Russell and co-workers studied solvent annealing and extraction as a means of producing vertically aligned cylinders throughout the film.[24,25] The influence of these factors on the structure formation, however, is a critical interplay between the χ parameters of the polymers and the solvent and is therefore strongly system-dependent.

CONCLUSION

In summary, we have synthesized a cylinder-forming diblock copolymer with a majority PSTPA phase exhibiting hole transport mobility and a minority PLA phase susceptible to soft selective etching. In thin films, we are able to introduce ~13 nm pores into the hole-transporting matrix by removal of PLA. Interestingly, a film-spanning pore structure is formed immediately after spin coating without the need for any alignment or annealing step. This self-assembled mesoporous hole-conducting film is a significant step toward self-assembled bulk heterojunction solar cell structures based on block copolymers. PSTPA microphase structures show promise for future device applications and are the subject of further research.

METHODS

Cyclic Voltammetry in Thin Films. Cyclic voltammetry was done in a typical three-electrode setup. The block copolymer was dissolved in toluene (concentration = 15 mg/mL) and deposited onto the platinum working electrode *via* spin coating. The CV experiments were performed at room temperature under argon atmosphere with a Ag/AgCl reference electrode and a platinum sheet as counter electrode in acetonitrile (with 0.1 M tetrabutylammonium hexafluorophosphate). Potentials were calibrated with the redox couple ferrocene/ferrocenium as external standard ($E_1^+/2$ (Fc^0/Fc$^+$) = 0.37 V *versus* Ag/AgCl). The setup was controlled by a JAISSLE BI-POT-PG 10 bipotentiostat, and the potential scans were performed with an AMEL Model 568 programmable function generator.

Charge Transport Measurements. Field-effect transistors (FETs) were fabricated in a bottom-gate bottom-contact configuration on highly doped Si wafers with a 300 nm thermally grown SiO_2 layer acting as gate dielectric. The freshly O_2 plasma-cleaned substrates were first treated with a hexamethyldisiloxane (HMDS) layer by sealing overnight in a glass vessel containing saturated HMDS vapor or alternatively soaked in a 1 mmol solution of octadecyltrichlorosilane (OTS) in cyclohexane for 30 min. Au source and drain electrodes were defined by standard photolithography (channel length L = 5 μm, width W = 10 mm). The FETs were characterized using a HP4155B semiconductor parameter analyzer. h-PSTPA films were deposited by spin coating from toluene and annealed for 12 h at 100 °C in a nitrogen atmosphere. Field-effect mobilities (μ_{FET}) were extracted from the saturated transfer characteristics employing eq 1, where I_{SD} is the source−drain current in the saturation regime, V_G and V_{SD} are the gate and source−drain voltages, C is the insulator capacitance, and V_0 is the threshold voltage.[26]

$$I_{SD} = \frac{W}{2L} C \mu_{FET} (V_G - V_0)^2 \qquad (1)$$

Thin Film Characterization. Copolymer films were formed by spin coating at 2000 rpm (accelaration 250 rpms^{-1}) from 10 wt % solutions in toluene onto silicon substrates coated with a 40 nm Au layer (thermally evaporated at 0.2 nm s^{-1} on a 2 nm Cr adhesion layer, rms surface roughness ≤1 nm for all wavelengths between 50 and 200 nm). Substrates were cleaned before spin coating by exposure to a CO_2 snowjet. The spin-coating chamber was purged with dry nitrogen flow at room temperature. The films were thermally annealed at 140 °C for up to 35 h under a nitrogen atmosphere. A cross-linked poly(dimethylsiloxane) (PDMS, Sylgard 184, Dow Corning) stamp was placed in contact with the surface of selected films during thermal annealing. The PLA minority component of the block copolymer was selectively degraded by immersing the films in 0.05 M NaOH$_{(aq)}$ solutions containing 40 vol% methanol. Ten minutes etching time was sufficient to obtain a fully porous structure in a 400 nm thick film.

Thin film microphase morphology was investigated by scanning force microscopy (SFM) (Nanoscope IV scanning force microscope, Digital Instruments 3100) in tapping mode with a silicon cantilever of resonant frequency 250−400 kHz). Transmission electron microscopy was conducted on a FEI Philips Tecnai 20 TEM, with an accelerating voltage of 200 keV (LaB$_6$ source filament). Cross-section samples for TEM were prepared by curing a drop of epoxy (Streurs epoxide) on top of the annealed polymer film protected by a 40 nm thermally evaporated gold layer. Immersing the sample in liquid nitrogen resulted in the epoxy drop cleaving from the silicon substrate, carrying the polymer film with it. Cross-section samples (≈50 nm thick) were prepared using an ultramictrome and stained by 10 min exposure to RuO$_4$ vapor in a sealed 4 mL vial containing 10 mg of RuCl$_3$ · 3H$_2$O powder in 1 mL of 15−20% NaOCl$_{(aq)}$.

Electrochemical Deposition. Electrochemical deposition of platinum was conducted potentiostatically in a standard three-electrode cell as described previously.[14] The copolymer film coated the working electrode with an active area of approximately 0.5 cm^2 defined by Kapton (DuPont) adhesive tape.

Supporting Information Available: Experimental procedures and characterization data for all new compounds. This material is available free of charge *via* the Internet at http://pubs.acs.org.

REFERENCES AND NOTES

1. Darling, S. B. Block Copolymers for Photovoltaics. *Energy Environ. Sci.* **2009**, *2*, 1266–1273.
2. Iovu, M.; Jeffries-El, M.; Sheina, E.; Cooper, J.; McCullough, R. Regioregular Poly(3- alkylthiophene) Conducting Block Copolymers. *Polymer* **2005**, *46*, 8582.
3. Müller, C.; Goffri, S.; Breiby, D. W.; Andreasen, J. W.; Chanzy, H. D.; Janssen, R. A. J.; Nielsen, M. M.; Radano, C. P.; Sirringhaus, H.; Smith, P.; *et al*. Tough, Semiconducting Polyethylene−Poly(3-hexylthiophene) Diblock Copolymers. *Adv. Funct. Mater.* **2007**, *17*, 2674–2679.
4. Dai, C.; Yen, W.; Lee, Y.; Ho, C.; Su, W. Facile Synthesis of Well-Defined Block Copolymers Containing Regioregular Poly(3-hexyl thiophene) *via* Anionic Macroinitiation Method and Their Self-Assembly Behavior. *J. Am. Chem. Soc.* **2007**, *129*, 11036–11038.
5. Chen, X. L.; Jenekhe, S. A. Block Conjugated Copolymers: Towards Quantum-Well Nanostructures for Exploring Spatial Confinement Effects on Electronic, Optoelectronic, and Optical Phenomena. *Macromolecules* **1996**, *29*, 6189–6192.
6. Lindner, S. M.; Hüttner, S.; Chiche, A.; Thelakkat, M.; Krausch, G. Charge Separation at Self-Assembled Nanostructured Bulk Interface in Block Copolymers. *Angew. Chem., Int. Ed.* **2006**, *45*, 3364–3368.
7. Tu, G.; Li, H.; Forster, M.; Heiderhoff, R.; Balk, L. J.; Scherf, U. Conjugated Triblock Copolymers Containing Both Electron-Donor and Electron-Acceptor Blocks. *Macromolecules* **2006**, *39*, 4327–4331.
8. Zhang, C.; Choi, S.; Haliburton, J.; R. Li, T. C.; Sun, S.; Ledbetter, A.; Bonner, C. E. Design, Synthesis and Characterization of a Donor−Bridge−Acceptor−Bridge Type Block Copolymer *via* Alkoxy and Sulfone Derivatized

Poly(phenylenevinylenes). *Macromolecules* **2006**, *39*, 4317–4326.

9. Sommer, M.; Lindner, S. M.; Thelakkat, M. Microphase-Separated Donor−Acceptor Diblock Copolymers: Influence of HOMO Energy Levels and Morphology on Polymer Solar Cells. *Adv. Funct. Mater.* **2007**, *17*, 1493–1500.

10. Sun, S. S.; Zhang, C.; Ledbetter, A.; Choi, S.; Seo, K.; Bonner, C. E.; Drees, M.; Sariciftci, N. S. Photovoltaic Enhancement of Organic Solar Cells by a Bridged Donor−Acceptor Block Copolymer Approach. *App. Phys. Lett.* **2007**, *90*, 043117.

11. Sommer, M.; Lang, A.; Thelakkat, M. Crystalline−Crystalline Donor−Acceptor Block Copolymers. *Angew. Chem., Int. Ed.* **2008**, *47*, 7901–7904.

12. Richard, F.; Brochon, C.; Leclerc, N.; Eckhardt, D.; Heiser, T.; Hadziioannou, G. Design of a Linear Poly(3-hexylthiophene)/Fullerene-Based Donor−Acceptor Rod−Coil Block Copolymer. *Macromol. Rapid Commun.* **2008**, *29*, 885–891.

13. Crossland, E.; Nedelcu, M.; Ducati, C.; Ludwigs, S.; Hillmyer, M.; Steiner, U.; Snaith, H. Block Copolymer Morphologies in Dye-Sensitized Solar Cells: Probing the Photovoltaic Structure−Function Relation. *Nano Lett.* **2009**, *9*, 2813–2819.

14. Crossland, E. J. W.; Kamperman, M.; Nedelcu, M.; Ducati, C.; Wiesner, U.; Smilgies, D. M.; Toombes, G. E. S.; Hillmyer, M. A.; Ludwigs, S.; Steiner, U.; *et al.* A Bicontinuous Double Gyroid Dye-Sensitized Solar Cell. *Nano Lett.* **2009**, *9*, 2807–2812.

15. Boudouris, B. W.; Frisbie, C. D.; Hillmyer, M. A. Nanoporous Poly(3-Alkylthiophene) Thin Films Generated from Block Copolymer Templates. *Macromolecules* **2008**, *41*, 67–75.

16. Botiz, I.; Darling, S. Self-Assembly of Poly(3-hexylthiophene)-*Block*-Polylactide Block Copolymer and Subsequent Incorporation of Electron Acceptor Material. *Macromolecules* **2009**, *42*, 8211–8217.

17. Choi, K.; Yoo, S.; Sung, Y.; Zentel, R. High Contrast and Rapid Switching Organic Polymeric Electrochromic Thin Films Based on Triarylamine Derivatives from Layer-by-Layer Assembly. *Chem. Mater.* **2006**, *18*, 5823–5825.

18. Snaith, H. J.; Whiting, G. L.; Sun, B.; Greenham, N. C.; Huck, W. T. S.; Friend, R. H. Self-Organization of Nanocrystals in Polymer Brushes. Application in Heterojunction Photovoltaic Diodes. *Nano Lett.* **2005**, *5*, 1653–1657.

19. Whiting, G. L.; Snaith, H. J.; Khodabakhsh, S.; Andreasen, J. W.; Breiby, D. W.; Nielsen, M. M.; Greenham, N. C.; Friend, R. H.; Huck, W. T. S. Enhancement of Charge-Transport Charateristics in Polymeric Films Using Polymer Brushes. *Nano Lett.* **2006**, *6*, 573–578.

20. Zalusky, A. S.; Olayo-Valles, R.; Wolf, J. H.; Hillmyer, M. A. Ordered Nanoporous Polymers from Polystyrene−Polylactide Block Copolymers. *J. Am. Chem. Soc.* **2002**, *124*, 12761–12773.

21. Crossland, E. J. W.; Ludwigs, S.; Hillmyer, M. A.; Steiner, U. Freestanding Nanowire Arrays from Soft-Etch Block Copolymer Templates. *Soft Matter* **2007**, *3*, 94–98.

22. Fehervari, A.; Kagumba, L.; Hadjikyriacou, S.; Chen, F.; Gaudiana, R. Photoluminescence and Excimer Emission of Functional Groups in Light Emitting Polymers. *J. Appl. Polym. Sci.* **2003**, *87*, 5823–5825.

23. Seo, E.; Nelson, R.; Fritsch, J.; Marcoux, L.; Leedy, D.; Adams, R. Anodic Oxidation Pathways of Aromatic Amines. Electrochemical and Electron Paramagnetic Resonance Studies. *J. Am. Chem. Soc.* **1966**, *88*, 3498–3503.

24. Lin, Z.; Kim, D. H.; Wu, X.; Booshahda, L.; Stone, D.; LaRose, L.; Russell, T. P. A Rapid Route to Arrays of Nanostructures in Thin Films. *Adv. Mater.* **2002**, *14*, 1373–1376.

25. Kim, S. H.; Misner, M. J.; Xu, T.; Kimura, M.; Russell, T. P. Highly Oriented and Ordered Arrays from Block Copolymers *via* Solvent Evaporation. *Adv. Mater.* **2004**, *16*, 226.

26. Dimitrakopoulos, C. D.; Malenfant, P. R. L. Organic Thin Film Transistors for Large Area Electronics. *Adv. Mater.* **2002**, *14*, 99.